



Mixed Convection Boundary Layer Flow over a Horizontal Circular Cylinder in Al_2O_3-Ag /Water Hybrid Nanofluid with Viscous Dissipation

Eddy Elfiano^{1,2}, Nik Mohd Izual Nik Ibrahim^{2,*}, Muhammad Khairul Anuar Mohamed³

¹ Department of Mechanical Engineering, Faculty of Engineering Universitas Islam Riau, 28284 Pekanbaru, Provinsi Riau, Indonesia

² Faculty of Engineering and Technology, DRB-HICOM University of Automotive Malaysia, DRB-HICOM Automotive Complex, Lot 1449, PT 2204, Peramu Jaya Industrial Area, 26607 Pekan, Pahang Darul Makmur, Malaysia

³ Centre for Mathematical Sciences Universiti Malaysia Pahang, Lebuhraya Persiaran Tun Khalil Yaakob, 26300 Kuantan, Pahang, Malaysia

ARTICLE INFO

Article history:

Received 13 July 2023

Received in revised 15 August 2023

Accepted 17 September 2023

Available online 1 January 2024

Keywords:

Mixed convection; hybrid nanofluid; circular cylinder; viscous dissipation

ABSTRACT

This paper investigated the mathematical modelling for mixed convection boundary layer flow over a horizontal circular cylinder in Al_2O_3-Ag /water hybrid nanofluid with viscous dissipation. The transformed partial differential equations (PDEs) are numerically solved using an implicit finite-difference approach known as the Keller-box method. The numerical solutions for the reduced Nusselt number, $Nu_x Re_x^{-1/2}$, local skin friction coefficient, $C_f Re_x^{1/2}$, temperature profile, $\theta(y)$ and velocity profiles $f'(y)$ are found and graphically presented in detail. Effects of the Eckert number, Richardson number and nanoparticle volume fraction are all examined and explained. It is found that the increase of volume fraction of nano material in nanofluid has increased the value of skin friction coefficient. The low density of nano oxides such as alumina in hybrid nanofluids also contribute to reduce friction between fluid and body surface. Based on numerical analysis, the combination of nanoparticles in the form of Al_2O_3-Ag /water hybrid nanofluid may reduce skin friction phenomena while sustaining heat transfer characteristics comparable to Ag /water nanofluid. The results in this paper are original and will assist researchers working in the field of boundary layer flow. It can also be utilised as a reference in experimental studies to reduce operating costs.

1. Introduction

Nanotechnology is used in many engineering applications to dissipate heat. The primary objective is to improve heat transfer in engineering devices such as heat exchangers and engine cooling systems. The thermal conductivity of fluids commonly used in heat transfer, such as water and ethylene glycol, is considered inadequate at both the fluid and air surfaces. As a result, the heat transfer rate in a car radiator must be increased, requiring the development of innovative heat transfer fluids [1]. However, Nano-coolants are a new class of coolants developed as a result of the most recent developments in science [2]. In 1995, Choi from Argonne National Laboratory introduced

* Corresponding author.

E-mail address: izual@dhu.edu.my (Nik Mohd Izual Nik Ibrahim)

the concept of "nanofluids", which indicate the stable suspension produced by suspending metal, metallic oxide, or non-metallic nanoparticles with average diameters of less than 100 nm in a base fluid [3]. Nanofluid has potential in thermal management systems such as liquid-submerged cooling for transformers and electronic circuit boards, due to its successful engine downsizing implementation in the automotive industry [4].

Metal nanoparticles have been recognized for their superior heat transfer capabilities compared to oxide nanoparticles, due to their thermal conductivity, density, and specific heat characteristics. The use of nanofluids has been experimentally proven to enhance many thermal properties, including thermal conductivity, thermal diffusivity, viscosity, and convective heat transfer, as compared to conventional base fluids like water and oil [5]. As a lubricant additional, nanoparticle additives like CuO (copper oxide), MoS_2 (molybdenum disulfide), and TiO_2 (titanium dioxide) can be used to minimize friction and wear [6]. Using a water-based fluid, three distinct types of nanoparticles are considered: Cu , Al_2O_3 , and TiO_2 . It is shown that an increase in the volume fraction of each distinct nanoparticle results in a corresponding rise in both the skin friction coefficient and heat transfer rate at the surface [7].

Numerous investigations have been done by researchers to examine the movement of fluids within a circular cylinder, Tham *et al.*, [8] and Mohamed *et al.*, [9] who have investigated mixed convection over a horizontal circular cylinder have seen an increase in the skin friction coefficient at the middle of the cylinder (1.1-1.5 radians) before falling towards the cylinder's end surface. Based on a review of the literatures and the opinions of certain researchers, focus on Newtonian heating by Salleh *et al.*, [10], the flow of Jeffrey fluid by Zokri *et al.*, [11], flow past a symmetric cylinder by Mahat *et al.*, [12], nanofluid by Tham *et al.*, [13], flow of viscoelastic fluid by Widodo *et al.*, [14]. Following that, the flow and heat transfer are immersed in a viscoelastic nanofluid by Mahat *et al.*, [15]. The results indicate that an increase in the mixed convection parameter results to an increase in skin friction values, while Nusselt number values exhibit the opposite trend.

Recent research has been conducted on the phenomenon of fluid flow on a horizontal circular cylinder in a hybrid nanofluid. Notably, the works of Roy and Akter have contributed to this field of research [16] who reported that Al_2O_3-Cu /water in the form of hybrid nanofluid increases heat transfer by approximately 28.28% when compared to Al_2O_3 -water in the form of nanofluid and by approximately 51.15% when compared to pure fluid. The properties of a hybrid nanofluid including two nanoparticles CuO and either Au or Al differ significantly from those of a nanofluid containing only one component CuO by Alwawi *et al.*, [17].

Based on the articles mentioned above that have been reviewed, It is noteworthy to mention that convective heat transfer on a circular cylinder is still an interesting topic to explore. Therefore, the purpose of the present study is to investigate the mixed convection boundary layer flow over a horizontal circular cylinder in Al_2O_3-Ag /water hybrid nanofluid with viscous dissipation. The governing Partial Differential Equations (PDEs) are solved using numerical methods, and the investigation of the fluctuation of relevant physical parameters has not been previously conducted, hence, the findings presented in this study are original.

2. Mathematical Formulations

The object under consideration is a horizontal circular cylinder (HCC) with a given radius a , which is heated to a constant temperature T_w embedded in a hybrid nanofluid with ambient temperature T_∞ . Figure 1 show the physical representation of the case. The orthogonal coordinates of \bar{x} is measured along the cylinder surface. Starting from the lower stagnation point $\bar{x} = 0$, and \bar{y} calculates the distance normal to the surface. The boundary layer approximation is valid, the dimensional

governing equations of steady mixed convection boundary layer flow are taken from the previous study [18, 19]:

$$\frac{\partial \bar{u}}{\partial \bar{x}} + \frac{\partial \bar{v}}{\partial \bar{y}} = 0, \quad (1)$$

$$\bar{u} \frac{\partial \bar{u}}{\partial \bar{x}} + \bar{v} \frac{\partial \bar{u}}{\partial \bar{y}} = \bar{u}_e \frac{d\bar{u}_e}{d\bar{x}} + \frac{\mu_{hnf}}{\rho_{hnf}} \frac{\partial^2 \bar{u}}{\partial \bar{y}^2} + \frac{(\rho\beta)_{hnf}}{\rho_{hnf}} g(T - T_\infty) \sin \frac{\bar{x}}{a}, \quad (2)$$

$$\bar{u} \frac{\partial T}{\partial \bar{x}} + \bar{v} \frac{\partial T}{\partial \bar{y}} = \frac{k_{hnf}}{(\rho C_p)_{hnf}} \frac{\partial^2 T}{\partial \bar{y}^2} + \frac{\mu_{hnf}}{(\rho C_p)_{hnf}} \left(\frac{\partial \bar{u}}{\partial \bar{y}} \right)^2, \quad (3)$$

subjected to the boundary condition:

$$\bar{u}(\bar{x}, 0) = \bar{v}(\bar{x}, 0) = 0, \quad T(\bar{x}, 0) = T_w, \quad (4)$$

$$\bar{u}(\bar{x}, \infty) \rightarrow \bar{u}_e, \quad T(\bar{x}, \infty) \rightarrow T_\infty,$$

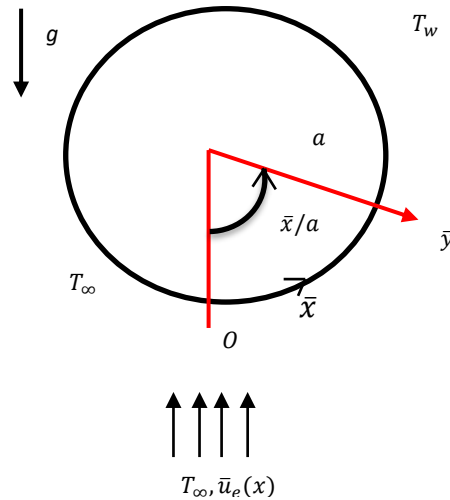


Fig. 1. Physical model of the coordinate system for mixed convection [20]

Where \bar{u} and \bar{v} represent the velocity components along the \bar{x} and \bar{y} axes, respectively. \bar{u}_e is external velocity. The symbol μ_{hnf} represents the dynamic viscosity of a hybrid nanofluid, while ρ_{hnf} denotes the density of the hybrid nanofluid. The variable g represents the acceleration due to gravity, β_{hnf} represents the thermal expansion coefficient of the hybrid nanofluid, T represents the local temperature, $(\rho C_p)_{hnf}$ is the heat capacity of hybrid nanofluid, ν_{hnf} is the kinematic viscosity of hybrid nanofluid and k_{hnf} is the thermal conductivity of hybrid nanofluid which can be expressed from the previous study [18, 21, 22]:

$$\nu_{hnf} = \frac{\mu_{hnf}}{\rho_{hnf}}, \quad \mu_{hnf} = \frac{\mu_f}{(1 - \phi_1)^{2.5}(1 - \phi_2)^{2.5}},$$

$$\rho_{hnf} = (1 - \phi_2)[(1 - \phi_1)\rho_f + \phi_1\rho_{s1}] + \phi_2\rho_{s2},$$

$$(\rho\beta)_{hnf} = (1 - \phi_2)[(1 - \phi_1)(\rho\beta)_f + \phi_1(\rho\beta)_{s1}] + \phi_2(\rho\beta)_{s2},$$

$$(\rho C_p)_{hnf} = (1 - \phi_2)[(1 - \phi_1)(\rho C_p)_f + \phi_1(\rho C_p)_{s1}] + \phi_2(\rho C_p)_{s2},$$

$$\frac{k_{hnf}}{k_{bf}} = \frac{k_{s2} + 2k_{bf} - 2\phi_2(k_{bf} - k_{s2})}{k_{s2} + 2k_{bf} + \phi_2(k_{bf} - k_{s2})}, \quad \frac{k_{bf}}{k_f} = \frac{k_{s1} + 2k_f - 2\phi_1(k_f - k_{s1})}{k_{s1} + 2k_f + \phi_1(k_f - k_{s1})}$$

The subscript $hnf, f, s1$ and $s2$ denote the physical characteristics of a hybrid nanofluid, base fluid, alumina Al_2O_3 nanoparticle, and silver Ag nanoparticle, respectively. In this study, initially 0.06 vol. solid nanoparticle of Ag ($\phi_2 = 0.06$) is added into water-based fluid to form Ag /water nanofluid. In the meantime, 0.1 vol. solid nanoparticle of Al_2O_3 ($\phi_1 = 0.1$) is added to the Ag /water nanofluid to create the Al_2O_3 - Ag /water hybrid nanofluid.

The governing dimensionless variables are presented:

$$\begin{aligned} x &= \frac{\bar{x}}{a}, & y &= Re^{1/2} \frac{\bar{y}}{a}, \\ u &= \frac{\bar{u}}{u_\infty}, & v &= Re^{1/2} \frac{\bar{v}}{u_\infty}, \end{aligned} \quad (5)$$

$$\theta(\eta) = \frac{T - T_\infty}{T_w - T_\infty}, \quad \bar{u}_e(x) = u_\infty \sin\left(\frac{\bar{x}}{a}\right), \quad u_e(x) = \frac{\bar{u}_e(x)}{u_\infty} = \sin x.$$

Using Eq. (5), Eq. (1) - Eq. (3) becomes

$$\frac{\partial u}{\partial x} + \frac{\partial v}{\partial y} = 0, \quad (6)$$

$$u \frac{\partial u}{\partial x} + v \frac{\partial u}{\partial y} = u_e \frac{du_e}{dx} + \frac{v_{hnf}}{v_f} \frac{\partial^2 u}{\partial y^2} + \frac{(\rho\beta)_{hnf}}{\rho_{hnf}\beta_f} \lambda \theta \sin x, \quad (7)$$

$$u \frac{\partial \theta}{\partial x} + v \frac{\partial \theta}{\partial y} = \frac{k_{hnf}}{v_f(\rho C_p)_{hnf}} \frac{\partial^2 \theta}{\partial y^2} + \frac{v_{hnf}}{v_f} \frac{\rho_{hnf}(C_p)_f}{(\rho C_p)_{hnf}} Ec \left[\frac{\partial u}{\partial y} \right]^2, \quad (8)$$

Subject to boundary conditions:

$$u(x, 0) = 0, \quad v(x, 0) = 0, \quad \theta(x, 0) = 1, \quad (9)$$

$$u(x, \infty) \rightarrow u_e, \quad \theta(x, \infty) \rightarrow 0,$$

Where θ is the rescale dimensionless temperature of the hybrid nanofluid and Gr, Re, Ec and λ are the Grashof, Reynold, Eckert, and Richardson numbers, respectively.

$$Gr = \frac{g\beta_f(T_w - T_\infty)a^3}{v_f^2}, \quad Re = \frac{u_\infty a}{v_f}, \quad Ec = \frac{v_f^2 Gr}{a^2(C_p)_f(T_w - T_\infty)}, \quad \lambda = \frac{Gr}{Re^2}.$$

In order to solve Eq. (6) – (8), the following function are introduced:

$$\psi = xf(x, y), \quad \theta = \theta(x, y), \quad (10)$$

Where ψ is the stream function which defined as;

$$u = \frac{\partial \psi}{\partial y} \quad \text{and} \quad v = -\frac{\partial \psi}{\partial x}$$

Substituting Eq. (10) into Eq. (6) - Eq. (8), the following partial differential equations (PDEs) are obtained the momentum and energy equations:

$$\frac{v_{hnf}}{v_f} \frac{\partial^3 f}{\partial y^3} + f \frac{\partial^2 f}{\partial y^2} - \left[\frac{\partial f}{\partial y} \right]^2 + \frac{(\rho\beta)_{hnf}}{\rho_{hnf}\beta_f} \frac{\sin x}{x} (\lambda\theta + \cos x) = x \left[\frac{\partial f}{\partial y} \frac{\partial^2 f}{\partial x \partial y} - \frac{\partial f}{\partial x} \frac{\partial^2 f}{\partial y^2} \right] \quad (11)$$

$$\frac{k_{hnf}(\rho C_p)_f}{k_f(\rho C_p)_{hnf}} \frac{1}{Pr} \frac{\partial^2 \theta}{\partial y^2} + f \frac{\partial \theta}{\partial y} = x \left[\frac{\partial f}{\partial y} \frac{\partial \theta}{\partial x} - \frac{\partial f}{\partial x} \frac{\partial \theta}{\partial y} \right] - \left[xEc \frac{v_{hnf}}{v_f} \frac{\rho_{hnf}(C_p)_f}{(\rho C_p)_{hnf}} \left(\frac{\partial^2 f}{\partial y^2} \right)^2 \right] \quad (12)$$

Where $Pr = \frac{v_f(\rho C_p)_f}{k_f}$ is the Prandtl number. Other quantities are detailed as follows:

$$\begin{aligned} i. \quad \frac{v_{hnf}}{v_f} &= \frac{1}{(1 - \phi_1)^{2.5}(1 - \phi_2)^{2.5}(1 - \phi_2)[(1 - \phi_1) + \phi_1(\rho_{s1}/\rho_f)] + \phi_2(\rho_{s2}/\rho_f)} \\ ii. \quad \frac{(\rho\beta)_{hnf}}{\rho_{hnf}\beta_f} &= \frac{(1 - \phi_2)[(1 - \phi_1)\rho_f + \phi_1(\rho\beta)_{s1}/\beta_f] + \phi_2(\rho\beta)_{s2}/\beta_f}{(1 - \phi_2)[(1 - \phi_1)\rho_f + \phi_1\rho_{s1}] + \phi_2\rho_{s2}} \\ iii. \quad \frac{k_{hnf}(\rho C_p)_f}{k_f(\rho C_p)_{hnf}} &= \frac{k_{hnf}/k_f}{(1 - \phi_2)[(1 - \phi_1) + \phi_1(\rho C_p)_{s1}/(\rho C_p)_f] + \phi_2(\rho C_p)_{s2}/(\rho C_p)_f} \\ iv. \quad \frac{\rho_{hnf}(C_p)_f}{(\rho C_p)_{hnf}} &= \frac{(1 - \phi_2)[(1 - \phi_1)\rho_f + \phi_1\rho_{s1}] + \phi_2\rho_{s2}}{(1 - \phi_2)[(1 - \phi_1)\rho_f + \phi_1(\rho C_p)_{s1}/(C_p)_f] + \phi_2(\rho C_p)_{s2}/(C_p)_f} \end{aligned}$$

The boundary conditions Eq. (9) become:

$$f(x, 0) = \frac{\partial f}{\partial y}(x, 0) = 0, \quad \theta(x, 0) = 1, \quad (13)$$

$$\frac{\partial f}{\partial y}(x, \infty) \rightarrow \frac{\sin x}{x}, \quad \theta(x, \infty) \rightarrow 0$$

The physical quantities of interest are the local Nusselt number Nu_x and the skin friction coefficient C_f , which are given by:

$$Nu_x = \frac{aq_w}{k_f(T_w - T_\infty)}, \quad C_f = \frac{\tau_w}{\rho_f u_\infty^2} \quad (14)$$

The surface shear stress τ_w and the surface heat flux q_w are given by

$$\tau_w = \mu_{hnf} \left[\frac{\partial \bar{u}}{\partial \bar{y}} \right]_{\bar{y}=0}, \quad q_w = -k_{hnf} \left[\frac{\partial T}{\partial \bar{y}} \right]_{\bar{y}=0}, \quad (15)$$

with k being the thermal conductivity. Using Eq. (5) and Eq. (10) give

$$C_f Re_x^{1/2} = \frac{1}{(1-\phi_1)^{2.5}(1-\phi_2)^{2.5}} \left(x \frac{\partial^2 f}{\partial y^2} \right)_{\bar{y}=0} \quad \text{and} \quad Nu_x Re_x^{1/2} = -\frac{k_{hnf}}{k_f} \left(\frac{\partial \theta}{\partial y} \right)_{\bar{y}=0} \quad (16)$$

Furthermore, the velocity profile and temperature distributions can be obtained from the following relations:

$$u = f'(x, y), \quad \theta = \theta(x, y) \quad (17)$$

3. Methodology

Using the Keller-box method, the partial differential equations (PDEs) Eq. (11) and Eq. (12) with boundary condition Eq. (13) are numerically solved. Keller-box method is an effective implicit technique for solving non-linear parabolic partial differential equations (PDEs). This study employs the use of a nonlinear equation to solve heat flow problems. Na [23], Cebeci and Cousteix [24], and recently Mohamed [25], each source offers detailed explanations of the research methods used. Keller-box method involves the following four steps. The first step involves the reduction of the Partial Differential Equations (PDEs) subjected to the boundary conditions to a first-order system. The central finite difference approach is employed, and The Newton's method is used to linearize the given function. The algebraic equations obtained are then transformed into a matrix-vector form, and lastly, the technique of block tridiagonal elimination is used to solve them. The algorithm is coded into MATLAB program to numerically compute. To obtain accurate numerical findings, noting that the thickness of the boundary layer satisfied $y_\infty = 7 - 10$ with step size $\Delta y = 0.02$, $\Delta x = 0.005$ are used.

4. Results

Eq. (11) and Eq. (12) represent momentum and energy respectively, based on a number of parameters, namely Prandtl number Pr , Richardson number λ , Eckert number Ec and the quantities of hybrid nanofluid. The comparison values of the reduce Nusselt number, $Nu_x Re_x^{-1/2}$ on the surface body have been computed. It is found that a very strong correlation between the findings of three researchers. Table 1 shows the values of thermophysical properties of water and nanoparticles [25, 26]. Table 2 presents the comparison between the present results with the previously reported results by Merkin [27], Nazar [28] and Mohamed [29] for various value of the Richardson number λ when $\phi_1 = \phi_2 = Ec = 0$ and $Pr = 1$. Also, it is discovered that they are in agreement. Table 3 and 4 present the values of reduce Nusselt number, $Nu_x Re_x^{-1/2}$ and reduce of skin friction, $C_f Re_x^{1/2}$ respectively for various values of circular cylinder x and Richardson number λ when $Pr = 7$ and $Ec = 0.1$.

Table 1
 Thermophysical properties of water and nanoparticles [24, 25]

Physical properties	Water (f)	Al_2O_3 (ϕ_1)	Ag (ϕ_2)	TiO_2	Cu
ρ (kg/m ³)	997	3970	10500	4250	8933
Cp (J/kg.K)	4179	765	235	686.2	385
K (W/m.K)	0.613	40	429	8.95	400

Table 2
 Comparison value of $Nu_x Re_x^{-1/2}$ with previous published results for different values of x and λ when $\phi_1 = \phi_2, Pr = 1, Ec = 0$

x/λ	-1.0				0				1.0			
	Merkin [27]	Nazar [28]	Mohamed [29]	Present	Merkin [27]	Nazar [28]	Mohamed [29]	Present	Merkin [27]	Nazar [28]	Mohamed [29]	Present
0.0	0.5067	0.5080	0.5067	0.5067	0.5705	0.5710	0.5705	0.5705	0.6156	0.6160	0.6156	0.6156
0.2	0.5018	0.5022	0.5016	0.5015	0.5658	0.5658	0.5669	0.5668	0.6115	0.6125	0.6126	0.6125
0.4	0.4865	0.4862	0.4862	0.4859	0.5564	0.5564	0.5564	0.5562	0.6028	0.6031	0.6037	0.6036
0.6	0.4594	0.4584	0.4589	0.4584	0.5391	0.5391	0.5389	0.5387	0.5885	0.5880	0.5892	0.5889
0.8	0.4160	0.4140	0.4151	0.4144	0.5145	0.5145	0.5143	0.5139	0.5686	0.5673	0.5690	0.5687
1.0	0.3326	0.3259	0.3301	0.3280	0.4826	0.4808	0.4823	0.4817	0.5435	0.5414	0.5436	0.5432
1.2					0.4426	0.4406	0.4414	0.4414	0.5133	0.5105	0.5126	0.5126
1.4					0.3928	0.3909	0.3912	0.3912	0.4785	0.4750	0.4774	0.4774
1.6					0.3280	0.3262	0.3258	0.3257	0.4394	0.4354	0.4381	0.4380
1.8					0.2114	0.2049	0.2043	0.2039	0.3967	0.3924	0.3951	0.3950
2.0									0.3509	0.3465	0.3500	0.3491
2.2									0.3029	0.3002	0.3013	0.3012
2.4									0.2540	0.2515	0.2526	0.2524
2.6									0.2061	0.2040	0.2051	0.2048
2.8									0.1634	0.1636	0.1632	0.1628
3.0									0.1354	0.1397	0.1371	0.1358
π									0.1306	0.1380	0.1327	0.1317

Table 3
 Values of $Nu_x Re_x^{-1/2}$ with different values of x and λ when $Pr = 7$ and $Ec = 0.1$

x/λ	-1.0	-0.5	0.0	0.5	1.0	2.0
0.0	1.0974	1.1406	1.1786	1.2126	1.2436	1.2985
0.2	1.0808	1.1237	1.1609	1.194	1.2238	1.2761
0.4	1.0337	1.0761	1.1115	1.1418	1.1684	1.2131
0.6	0.9610	1.0038	1.0368	1.0633	1.0850	1.1178
0.8	0.8679	0.9147	0.9463	0.9686	0.9844	1.0025
1.0	0.7536	0.8152	0.8489	0.8682	0.8785	0.8807
1.2	0.5849	0.7057	0.7506	0.7708	0.7772	0.7650
1.4		0.5672	0.6511	0.6803	0.6869	0.6644
1.6			0.5375	0.5945	0.6087	0.5836
1.8			0.3193	0.5034	0.5384	0.5217
2.0				0.3790	0.4674	0.4743
2.2					0.3833	0.4341
2.4					0.2673	0.3944
2.6						0.3501
2.8						0.2981
3.0						0.2342
π						0.1676

Table 4

Values of $C_f Re_x^{1/2}$ with different values of x and λ when $Pr = 7$ and $Ec = 0.1$

x/λ	-1.0	-0.5	0.0	0.5	1.0	2.0
0.0	0	0	0	0	0	0
0.2	0.168	0.2064	0.2426	0.2770	0.3100	0.3728
0.4	0.3117	0.3895	0.4623	0.5314	0.5976	0.7231
0.6	0.4082	0.5278	0.6384	0.7428	0.8423	1.0305
0.8	0.4372	0.6034	0.7539	0.8943	1.0274	1.2776
1.0	0.3783	0.6023	0.7965	0.9742	1.1409	1.4519
1.2	0.1901	0.5132	0.7593	0.9766	1.1769	1.5464
1.4		0.3174	0.6402	0.9018	1.1362	1.5604
1.6			0.4372	0.7562	1.0257	1.4996
1.8			0.1008	0.5500	0.8585	1.3754
2.0				0.2900	0.6525	1.2041
2.2					0.4288	1.0045
2.4					0.2103	0.7959
2.6						0.5947
2.8						0.4100
3.0						0.2369
π						0.1043

Figure 2 illustrates the variation of volume fraction of hybrid nanofluids against reduce heat transfer along the body circular cylinder. It was observed that the effect of variation in ϕ_1 and ϕ_2 are more significantly at the stagnation point ($x = 0$). It is claimed that the reduce of heat transfer decreasing along a cylinder surface. The $Al_2O_3-Ag/water$ ($\phi_1 = 0.1, \phi_2 = 0.06$) hybrid nanofluid score highest values in reduce of heat transfer compared to water-based fluid and $Ag/water$ ($\phi_1 = 0.0, \phi_2 = 0.06$) nanofluid. These results are comparable with high-cost $Ag/water$ ($\phi_1 = 0.0, \phi_2 = 0.16$) nanofluid. The ability of the hybrid nanofluid, which combines metal and low-cost oxide nanoparticles, to transport heat to surfaces is demonstrated to be on par with that of premium metal nanofluid.

Figure 3 show that values of skin friction is typical at the stagnation region ($x = 0$). At this point, the nanoparticles have almost no effect on friction. As fluid flows through the cylinder body, the skin friction $C_f Re_x^{1/2}$ increases when 6 % vol. of Silver Ag nano material is added up into water-based fluid with the adding 10 % vol. of Alumina Al_2O_3 nano oxide to form the $Al_2O_3-Ag/water$ ($\phi_1 = 0.1, \phi_2 = 0.06$) hybrid nanofluid. From Figure 3, it was found that values of skin friction is unique and then increase again without adding nano oxide ($\phi_1 = 0.0$). The highest values of skin friction with adding 6 % and 16 % nano material to form the $Ag/water$ ($\phi_1 = 0.0, \phi_2 = 0.06$) and ($\phi_1 = 0.0, \phi_2 = 0.16$) nanofluid respectively. Considering $Al_2O_3-Ag/water$ hybrid nanofluid has a concentration of nano oxide 10% and nano metal 6%, the friction is less than 16% $Ag/water$ nanofluid. As a result, it is safer for the surface and increases its usefulness. Generally, the highest $C_f Re_x^{1/2}$ occurs when the fluid passes through the surface body of cylinder x between 1.0-1.5 radian.

The temperature profiles $\theta(y)$ and velocity profiles $f'(\eta)$ at stagnation region ($x = 0$) for various values of ϕ_1 and ϕ_2 are showed in Figure 4 and Figure 5, respectively. It is obvious that the presence of more nanoparticles has raised the thickness of the thermal boundary layer and decreasing the thickness of the velocity boundary layer. The addition of nanoparticles in hybrid nanofluid has increased the thermal conductivity of fluid, raising thermal diffusivity and increasing thermal boundary layer thickness. This is realistic especially for nano oxide has higher specific heat than nano material to store energy. Adding up nano oxide to $Ag/water$ to form the hybrid nanofluid will increase the thermal boundary layer thickness. It means, increasing of thermal boundary layer thickness will increase heat transfer.

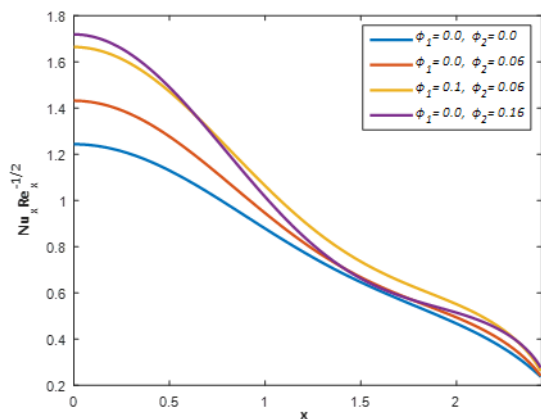


Fig. 2. Variation of $Nu_x Re_x^{-1/2}$ against x for various of volume fraction ϕ_1 and ϕ_2 When $Pr = 7$, $\lambda = 1$ and $Ec = 0.1$

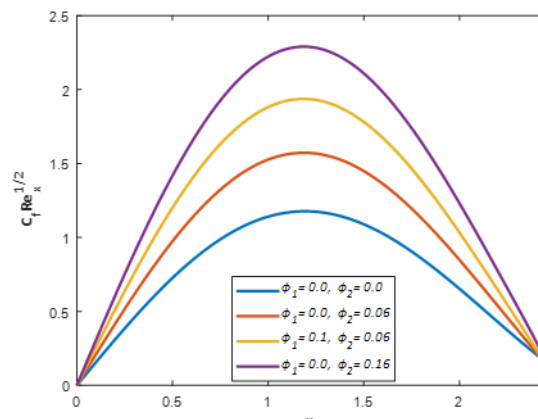


Fig. 3. Variation of $C_f Re_x^{1/2}$ against x for various of volume fraction ϕ_1 and ϕ_2 When $Pr = 7$, $\lambda = 1$ and $Ec = 0.1$

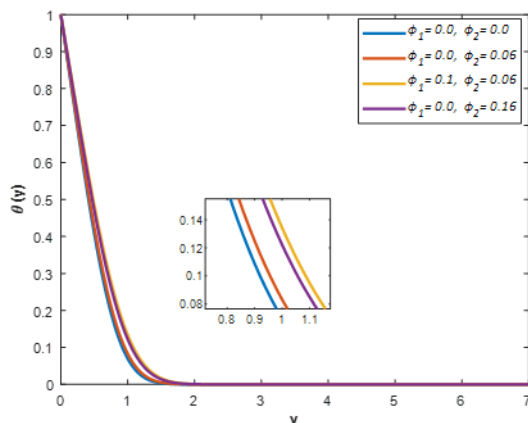


Fig. 4. Temperature profile $\theta(y)$ against y for various of volume fraction ϕ_1 and ϕ_2 When $Pr=7$, $\lambda = 1$ and $Ec=0.1$

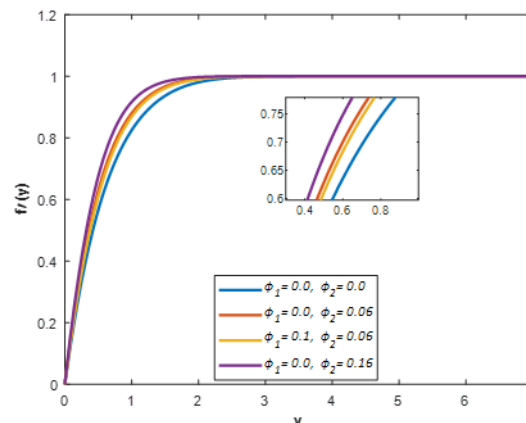


Fig. 5. Velocity profile $f'(y)$ against y for various of volume fraction ϕ_1 and ϕ_2 When $Pr = 7$, $\lambda = 1$ and $Ec = 0.1$

Next, Figures 6 and 7 show the variation reduce Nusselt number and reduce skin friction for various values of concentration of hybrid nanofluid when $Pr = 7$, $\lambda = 1$ and $Ec = 0.1$. Respectively. The flow and heat transfer performance of nano oxide Al_2O_3 and TiO_2 with Ag /water and Cu /water to form hybrid nanofluid. From the stagnation point, $x = 0$ to 0.7 radian, Ag /water transfer energy extremely well, next from 0.7 to 2.1 radian, Cu /Water dominates in transferring energy, lastly from 2.1 to 2.4 radian, Ag /water carries energy to completion (see Figure 6). This is due to the fact that the thermal conductivity of Ag and Al_2O_3 is larger than that of Cu and TiO_2 . According to James [30], The thermal conductivity is defined as ability of the substance to transfer energy. Figure 7, In general, the maximum $C_f Re_x^{1/2}$ is obtained when the fluid flows through the surface body of cylinder x between 1.0 and 1.5 . In comparison to Ag /water nanofluid and TiO_2 nano oxide, it was discovered that Cu /water nanofluid and Al_2O_3 nano oxide has a higher efficiency in reducing skin friction. This is due to the lower density of Cu and Al_2O_3 compared to Ag and TiO_2 .

The temperature $\theta(y)$ and velocity profiles $f'(\eta)$ at stagnation region ($x = 0$) for various concentration of hybrid nanofluid are showed in Figure 8 and Figure 9, respectively. In comparison to the hybrid nanofluids of Al_2O_3 - Cu /water, TiO_2 - Ag /water and and TiO_2 - Cu /water respectively,

the Figure 8 demonstrates that the Al_2O_3 -Ag/water hybrid nano fluid has an effective heat transfer beginning at 21.4% (1.5 radian) of the maximal boundary layer thickness on the surface. From Figure 9 show, in overall, the peak thickness of the velocity boundary layer occurs between 15% and 17% of the maximum thickness of the velocity boundary layer. The hybrid nanofluid of TiO_2 -Ag/water has a highest of velocity boundary layer thickness compare hybrid nanofluid of Al_2O_3 -Ag/water, Al_2O_3 -Cu/water and TiO_2 -Cu/water respectively. The effect of the density of a particle also impacts the thickness of the velocity boundary layer.

Lastly, Figure 10 and Figure 11 illustrate the Reduce Nusselt number and skin friction against x for various values of Eckert number. Both the figures agreed that the viscous dissipation effect Ec are negligible at stagnation region ($x = 0$). The viscous dissipation effect is more apparent near the middle of cylinder body. Increasing viscous dissipation of the Eckert number parameters decrease the temperature distribution with no significant change in the fluid velocity [31]. The highest Ec value indicates the low temperature distribution on the surface of the cylinder body and the Ec value also show no significant in reducing skin friction, both of the statements can be seen in Figure 10 and Figure 11 respectively.

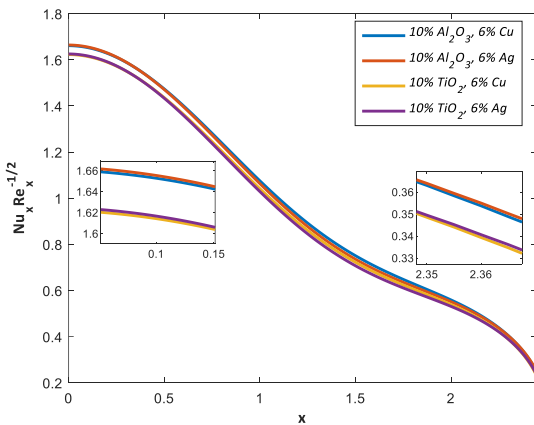


Fig. 6. Variation of $Nu_x Re_x^{-1/2}$ against x for various concentration of hybrid nanofluid When $Pr = 7$, $\lambda = 1$ and $Ec = 0.1$

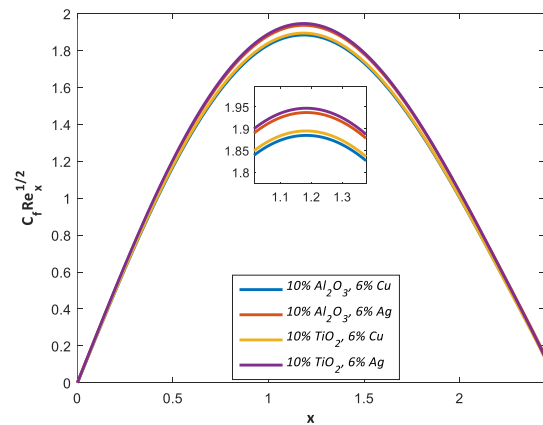


Fig. 7. Variation of $C_f Re_x^{1/2}$ against x for various concentration of hybrid nanofluid When $Pr = 7$, $\lambda = 1$ and $Ec = 0.1$

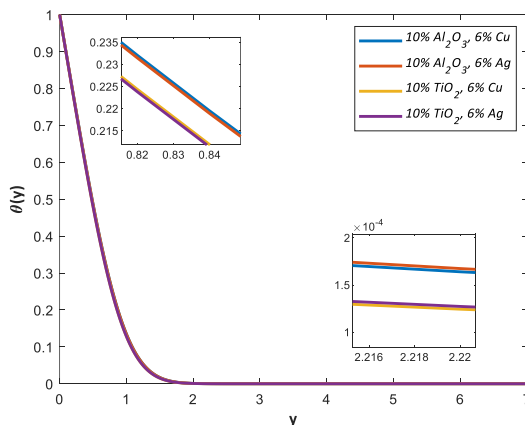


Fig. 8. Variation of temperature profile against boundary layer thickness for various concentration of hybrid nanofluid When $Pr = 7$, $\lambda = 1$ and $Ec = 0.1$

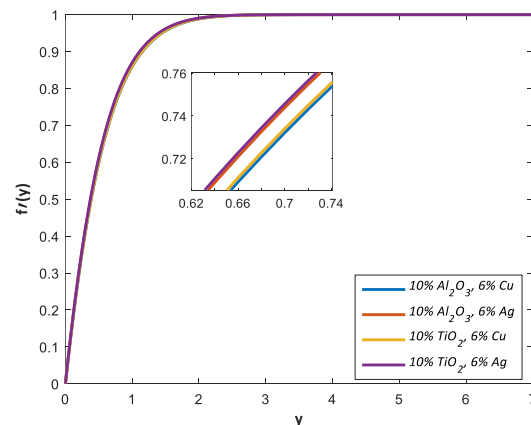


Fig. 9. Variation of velocity profile against boundary layer thickness for various concentration of hybrid nanofluid When $Pr = 7$, $\lambda = 1$ and $Ec = 0.1$

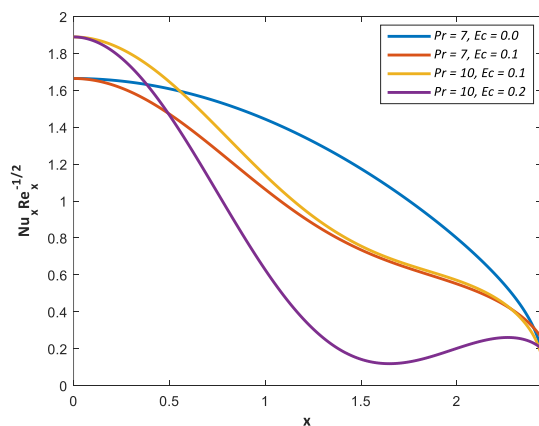


Fig. 10. Variation of $Nu_x Re_x^{-1/2}$ against x for various values of Ec , when $\lambda = 1$

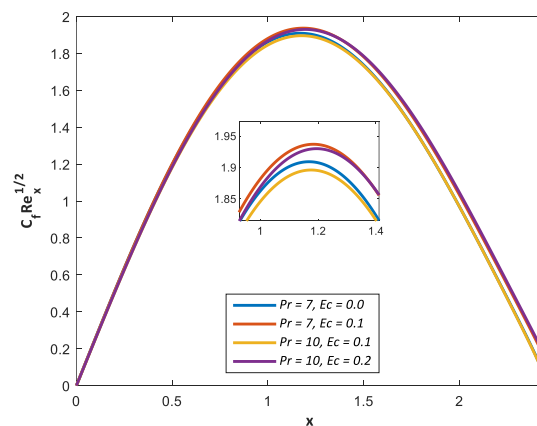


Fig. 11. Variation of $C_f Re_x^{1/2}$ against x for various values of Ec , when $\lambda = 1$

5. Conclusions

In this paper, the mixed convection boundary layer flow over a horizontal circular cylinder in hybrid nanofluid was investigated using the Keller-box method. The effects of the Richardson number λ , the Eckert number Ec , and the volume fractions of oxide nanoparticles and metal nanoparticles in hybrid nanofluid are documented. As a conclusion, it is found that the increase of volume fraction of nano material in nanofluid has increased the value of skin friction coefficient. In hybrid nanofluids, the low density of nano oxides such as alumina contributes to decrease friction between the fluid and body surface. The selection of nano oxide can be considered a reference for radiator coolant in automotive applications. The combination of nanoparticles in the form of Al_2O_3-Ag /water hybrid nanofluid may reduce skin friction phenomena while maintaining heat transfer characteristics comparable to Ag /water nanofluid, as determined by numerical investigation.

Following that, it is observed that skin friction encountered increased amounts of friction in the middle of the cylinder's surface, while the Nusselt number demonstrates a decreasing variation along the circular cylinder. An increase in the Eckert number results in a related rise in friction, at $x = 1.0$ to 1.5 on the surface of the cylinder, the greatest friction is evidently present. Although the skin friction effect is intended to have the opposite effect, an increase in Eckert number results in a decrease in Nusselt number.

Acknowledgement

Authors gratefully acknowledge the financial and facilities support from the Malaysia Ministry of Education (FRGS/1/2019/STG06/ DHUAM/02/1), DRB-HICOM University of Automotive Malaysia.

References

- [1] Leong, Kin Yuen, Rahman Saidur, S. N. Kazi, and A. H. Mamun. "Performance investigation of an automotive car radiator operated with nanofluid-based coolants (nanofluid as a coolant in a radiator)." *Applied Thermal Engineering* 30, no. 17-18 (2010): 2685-2692. <https://doi.org/10.1016/j.applthermaleng.2010.07.019>
- [2] Devireddy, Sandhya, Chandra Sekhara Reddy Mekala, and Vasudeva Rao Veeredhi. "Improving the cooling performance of automobile radiator with ethylene glycol water based TiO_2 nanofluids." *International communications in heat and mass transfer* 78 (2016): 121-126. <https://doi.org/10.1016/j.icheatmasstransfer.2016.09.002>
- [3] Choi, S. US, and Jeffrey A. Eastman. *Enhancing thermal conductivity of fluids with nanoparticles*. No. ANL/MSD/CP-84938; CONF-951135-29. Argonne National Lab.(ANL), Argonne, IL (United States), 1995.

- [4] Mohamed, Muhammad Khairul Anuar, Mohd Zuki Salleh, Fadhilah Che Jamil, and Ong Huei. "Free convection boundary layer flow over a horizontal circular cylinder in Al₂O₃-Ag/water hybrid nanofluid with viscous dissipation." *Malaysian Journal of Fundamental and Applied Sciences* 17, no. 1 (2021): 20-25. <https://doi.org/10.11113/mjfas.v17n1.1964>
- [5] Kakaç, Sadik, and Anchasa Pramuanjaroenkij. "Review of convective heat transfer enhancement with nanofluids." *International journal of heat and mass transfer* 52, no. 13-14 (2009): 3187-3196. <https://doi.org/10.1016/j.ijheatmasstransfer.2009.02.006>
- [6] Waqas, Muhammad, Rehan Zahid, Muhammad Usman Bhutta, Zulfiqar Ahmad Khan, and Adil Saeed. "A review of friction performance of lubricants with nano additives." *Materials* 14, no. 21 (2021): 6310. <https://doi.org/10.3390/ma14216310>
- [7] Tham, Leony, Roslinda Nazar, and Ioan Pop. "Mixed convection boundary layer flow from a horizontal circular cylinder in a nanofluid." *International Journal of Numerical Methods for Heat & Fluid Flow* 22, no. 5 (2012): 576-606. <https://doi.org/10.1108/09615531211231253>
- [8] Tham, Leony, Roslinda Nazar, and Ioan Pop. "Mixed convection flow from a horizontal circular cylinder embedded in a porous medium filled by a nanofluid: Buongiorno–Darcy model." *International Journal of Thermal Sciences* 84 (2014): 21-33. <https://doi.org/10.1016/j.ijthermalsci.2014.04.020>
- [9] Mohamed, Muhammad Khairul Anuar, Norhafizah Md Sarif, Nor Aida Zuraimi Md Noar, Mohd Zuki Salleh, and Anuar Mohd Ishak. "Mixed convection boundary layer flow on a horizontal circular cylinder in a nanofluid with viscous dissipation effect." *Malaysian Journal of Fundamental and Applied Sciences* 14, no. 1 (2018): 32-39. <https://doi.org/10.11113/mjfas.v14n1.803>
- [10] Salleh, Mohd Zuki, Roslinda Nazar, and Ioan Pop. "Mixed convection boundary layer flow over a horizontal circular cylinder with Newtonian heating." *Heat and Mass transfer* 46 (2010): 1411-1418. <https://doi.org/10.1007/s00231-010-0662-y>
- [11] Zokri, Syazwani Mohd, Nur Syamilah Arifin, Abdul Rahman Mohd Kasim, and Mohd Zuki Salleh. "Flow of jeffrey fluid over a horizontal circular cylinder with suspended nanoparticles and viscous dissipation effect: Buongiorno model." *CFD letters* 12, no. 11 (2020): 1-13. <https://doi.org/10.37934/cfdl.12.11.113>
- [12] Mahat, Rahimah, Sharidan Shafie, and Fatihhi Januddi. "Numerical analysis of mixed convection flow past a symmetric cylinder with viscous dissipation in viscoelastic nanofluid." *CFD letters* 13, no. 2 (2021): 12-28. <https://doi.org/10.37934/cfdl.13.2.1228>
- [13] Tham, Leony, Roslinda Nazar, and Ioan Pop. "Mixed convection flow over a horizontal circular cylinder with constant heat flux embedded in a porous medium filled by a nanofluid: Buongiorno–Darcy model." *Heat and Mass Transfer* 52 (2016): 1983-1991. <https://doi.org/10.1007/s00231-015-1720-2>
- [14] Widodo, Basuki, Chairul Imron, Nur Asiyah, Galuh Oktavia Siswono, and Tri Rahayuningsih. "Viscoelastic fluid flow pass a porous circular cylinder when the magnetic field included." *Far East Journal of Mathematical Sciences* 99, no. 2 (2016): 173-186. <https://doi.org/10.17654/MS099020173>
- [15] Mahat, Rahimah, Noraihan Afiqah Rawi, Abdul Rahman Mohd Kasim, and Sharidan Shafie. "Mixed convection flow of viscoelastic nanofluid past a horizontal circular cylinder with viscous dissipation." *Sains Malaysiana* 47, no. 7 (2018): 1617-1623. <https://doi.org/10.17576/jsm-2018-4707-33>
- [16] Roy, Nepal Chandra, and Aysha Akter. "Heat Transfer Enhancement and Boundary Layer Separations for a Hybrid Nanofluid Flow past an Isothermal Cylinder." *Journal of Applied and Computational Mechanics* 7, no. 4 (2021): 2096-2112. <https://doi.org/10.22055/JACM.2021.37795.3087>
- [17] Alwawi, Firas, Mohammed Swalmeh, Ibrahim Sulaiman, Nusayba Yaseen, Hamzeh Alkawasbeh, and Tarik Al Soub. "Numerical investigation of heat transfer characteristics for blood/water-based hybrid nanofluids in free convection about a circular cylinder." *Journal of Mechanical Engineering and Sciences* 16, no. 2 (2022): 8931-8942. <https://doi.org/10.15282/jmes.16.2.2022.10.0706>
- [18] Devi, Suriya Uma, and SP Anjali Devi. "Heat transfer enhancement of Cu–Al₂O₃/water hybrid nanofluid flow over a stretching sheet." *Journal of the Nigerian Mathematical Society* 36, no. 2 (2017): 419-433.
- [19] El-Zahar, E. R., A. M. Rashad, W. Saad, and L. F. Seddek. "Magneto-hybrid nanofluids flow via mixed convection past a radiative circular cylinder." *Scientific Reports* 10, no. 1 (2020): 10494. <https://doi.org/10.1038/s41598-020-66918-6>
- [20] Mohamed, Muhammad Khairul Anuar, Norhafizah Mohd Sarif, N. A. Z. M. Noar, Mohd Zuki Salleh, and Anuar Ishak. "Viscous dissipation effect on the mixed convection boundary layer flow towards solid sphere." *Trans. Sci. Technol* 3, no. 1-2 (2016): 59-67. <https://doi.org/10.11113/mjfas.v14n1.803>
- [21] Mohamed, Muhammad Khairul Anuar, Huei Ruey Ong, Hamzah Taha Alkawasbeh, and Mohd Zuki Salleh. "Heat transfer of ag-Al₂O₃/water hybrid nanofluid on a stagnation point flow over a stretching sheet with newtonian heating." In *Journal of Physics: Conference Series*, vol. 1529, no. 4, p. 042085. IOP Publishing, 2020. <https://doi.org/10.1088/1742-6596/1529/4/042085>

- [22] Abdullah, Nur Nazirah, Ahmad Nazri Mohamad Som, Norihan Md Arifin, and Aniza Ab Ghani. "The Effect of MHD on Marangoni Boundary Layer of Hybrid Nanofluid Flow Past a Permeable Stretching Surface." *CFD Letters* 15, no. 5 (2023): 65-73. <https://doi.org/10.37934/cfdl.15.5.6573>
- [23] Na, T. Y. *Computational Methods in Engineering Boundary Value Problems (Mathematics in Science and Engineering; V. 145)*. Elsevier, 1979.
- [24] Cousteix, T. Cebeci J., and J. Cebeci. "Modeling and computation of boundary-layer flows." *Berlin, Germany: Springer* (2005). https://doi.org/10.1007/3-540-27361-1_5
- [25] Zokri, Syazwani Mohd, Nur Syamilah Arifin, Muhammad Khairul Anuar Mohamed, Abdul Rahman Mohd Kasim, Nurul Farahain Mohammad, and Mohd Zuki Salleh. "Mathematical model of mixed convection boundary layer flow over a horizontal circular cylinder filled in a Jeffrey fluid with viscous dissipation effect." *Sains Malaysiana* 47, no. 7 (2018): 1607-1615. <https://doi.org/10.17576/jsm-2018-4707-32>
- [26] Das, Sarit K., Stephen US Choi, Wenhua Yu, and T. Pradeep. "Nanofluids-Science and Technology. A John Wiley & Sons." *Inc., Hoboken* (2008).
- [27] Merkin, J. H. "Mixed convection from a horizontal circular cylinder." *International journal of heat and mass transfer* 20, no. 1 (1977): 73-77. [https://doi.org/10.1016/0017-9310\(77\)90086-2](https://doi.org/10.1016/0017-9310(77)90086-2)
- [28] Nazar, Roslinda Mohd. "Mathematical models for free and mixed convection boundary layer flows of micropolar fluids." PhD diss., Universiti Teknologi Malaysia, 2004.
- [29] Mohamed, Muhammad Khairul Anuar, Mohd Zuki Salleh, N. A. Z. M. Noar, and Anuar Ishak. "The viscous dissipation effects on the mixed convection boundary layer flow on a horizontal circular cylinder." *Jurnal Teknologi* 78, no. 4-4 (2016): 73-79. <https://doi.org/10.11113/mjfas.v14n1.803>.
- [30] Speight, James G. *Natural gas: a basic handbook*. Gulf Professional Publishing, 2018. <https://doi.org/10.1016/C2015-0-02190-6>.
- [31] Famakinwa, O. A., O. K. Koriko, and K. S. Adegbe. "Effects of viscous dissipation and thermal radiation on time dependent incompressible squeezing flow of CuO– Al₂O₃/water hybrid nanofluid between two parallel plates with variable viscosity." *Journal of Computational Mathematics and Data Science* 5 (2022): 100062. <https://doi.org/10.1016/j.jcmds.2022.100062>.